

Nonisentropic Propagation of Sound in Uniform Ducts Using Euler Equations

R. S. Goonetilleke,* S. G. Lekoudis,† and W. C. Strahle‡

Georgia Institute of Technology, Atlanta, Georgia

The problem of sound propagation in uniform ducts is examined using the Euler equations. First, a numerical spatial marching technique is examined for the case of no mean flow. The technique uses an initial value formulation. It is found that the scheme is stability limited, in agreement with previous results obtained using the Helmholtz equation. Also duct mode analysis is performed and the following is observed. When the mean flow in the duct is treated as isentropic, the solutions agree with existing solutions. However, this implies no pressure gradient for the mean flow in the streamwise direction. If a mean pressure gradient is imposed, it is found that the lowest mode attenuates as it propagates against the flow direction. It is also found that the same mode grows due to an instability, if it propagates downstream. This instability is related to combustion instability.

Introduction

THE problem of sound propagation in uniform ducts has been of interest mainly due to the noise generated by the compressors of jet engines. However, lately, interest is also generated because of the instabilities present in ramjet combustors.¹

There are several other problems of interest when the issue is the instability observed in ramjets. Several questions that arise in this case are as follows: What happens when sound waves interact with vortical instabilities in the flow? Are the observed instabilities due to nonlinear sound effects or are they classical hydrodynamic instabilities? How does heat addition due to combustion affect the instabilities and to what extent is turbulence affected by them? How does the turbulence affect the instabilities?

Previous work²⁻⁵ has shown that the propagation of sound in uniform ducts reduces to an eigenvalue problem, with a single equation for the acoustic pressure. For a single frequency, multiple eigenvalues (modes) of propagation exist, corresponding to waves that travel both upstream and downstream in the duct. Depending on the conditions, these modes attenuate as they propagate (cut off) and this is purely an effect due to the geometry. None of these modes ever grows due to an instability. A basic assumption behind the work is that the mean flow in the duct is parallel and that the mean axial pressure gradient is zero. However, the axial pressure gradient is zero only if the effect of viscosity on the mean flow is neglected. As mentioned before, all of the computed eigenvalues showed that the wave mode propagates either with constant amplitude or, if the mode number is high enough, attenuates because of the geometry (cut off).

The practical problem involves the propagation of sound in variable area ducts. Different investigators used different perturbation methods and purely numerical methods to solve the problem.⁶⁻⁹ However, the existence of a mean pressure gradient in the mean flow is neglected in the lower-order approximation, usually called the zeroth-order problem in per-

turbation methods. Recent efforts using numerical methods are given in Refs. 10-14. These methods use finite element, finite difference, or wave envelope techniques and are directed toward the problem of ducts with large variations in their cross-sectional area.

In all of the works mentioned, the propagation of sound is treated as isentropic. This is satisfactory for the case of noise problems in jet engine ducts. However, there are cases (for example, a ramjet combustor) where the isentropic assumption of sound propagation becomes questionable. Previous work¹⁵ examined the one-dimensional problem of nonisentropic sound propagation. The classical combustion instability appears, where long wavelength waves with propagation speeds identical to the speed of sound exist, but with their amplitude growing due to an instability.

In what follows we re-examined the problem of sound propagation in uniform ducts. The motivation of this came from efforts to check solutions of the Euler equations for sound propagating in a duct with a backward-facing step, corresponding to the geometry of a ramjet combustor. We re-examined the piston problem by using a spatial marching technique, hoping that multimode propagation problems can be treated using this technique. An obvious restriction of the previous work on this problem is the assumption of "acoustic mean flow" in the duct. This means that the mean flow has constant pressure and is isentropic. If these assumptions are used, then the energy equation reduces to the isentropic relation for the sound wave. However, in order for this to be true, the streamwise pressure gradient for the mean flow has to be assumed as nonexistent, as it has been done in previous work related to duct acoustics. When this assumption is removed, the energy equation is modified and the eigenvalue problem has new solutions.

The mathematical formulation is in the next section. The discussion about the numerical methods follows and, finally, a section on results and discussion.

The Mathematical Formulation

Recent investigations of sound propagation use the Euler equations,^{13,14} together with finite difference techniques. In these investigations, the equations are solved using a time-marching procedure. Therefore, "steady state" is achieved when the acoustic field becomes periodic with the frequency imposed through a boundary condition. Motivation for using such an algorithm comes from the successes that the algorithm had with problems in fluid mechanics. The use of the Euler equations allows the computation of vortical in-

Received March 22, 1985; revision received Dec. 4, 1985. Copyright © American Institute of Aeronautics and Astronautics, Inc., 1986. All rights reserved.

*Graduate Research Assistant, School of Aerospace Engineering.

†Associate Professor, School of Aerospace Engineering. Member AIAA.

‡Regents Professor, School of Aerospace Engineering. Associate Fellow AIAA.

stabilities, when viscous effects on these instabilities can be neglected.

In order to be able to compute vortical instabilities and sound waves, the Euler equations are used in the present study. The geometry examined is shown in Fig. 1. The mean flow is assumed to be uniform in the x direction and the choice of the simple profile was made in order to compare with the previous results and also because this profile compares with the 1/7th power law profile.⁵ The variables used for nondimensionalizing the physical quantities are the ambient speed of sound \bar{c} , the half-duct width L , ambient temperature T_∞ , and the ambient fluid density $\bar{\rho}_\infty$. The pressure is made dimensionless using $\bar{\rho}_\infty \bar{c}^2$. The flow is assumed to consist of a steady mean flow and an unsteady disturbance corresponding to a sound wave. The disturbance is assumed to be periodic in time and the complex notation is introduced for convenience. Therefore, the flow quantities can be written as follows:

$$u = \bar{u}(x, y) + u'(x, y) \exp(i\theta') \quad (1a)$$

$$v = \bar{v}(x, y) + v'(x, y) \exp(i\theta') \quad (1b)$$

$$\rho = \bar{\rho}(x, y) + \rho'(x, y) \exp(i\theta') \quad (1c)$$

$$p = \bar{p}(x, y) + p'(x, y) \exp(i\theta') \quad (1d)$$

$$T = \bar{T}(x, y) + T'(x, y) \exp(i\theta') \quad (1e)$$

$$\theta' = \omega t \quad (1f)$$

where u and v denote the velocity components in the x and y direction, respectively, ρ the density, p the pressure, T the temperature, and ω the sound frequency.

In the above equations, the disturbance flow velocity components, pressure, density, and temperature are assumed to be composed of an amplitude function that depends on x and y and have a harmonic dependence on time with frequency ω . The mean flow quantities that are denoted by overbars are present in the absence of the acoustic wave and, therefore, satisfy the steady equations of motion by themselves. We will examine only the cases where there is no mean flow and where the mean flow is parallel. Obviously, the x momentum equation for a parallel mean flow dictates that the mean pressure gradient is independent of x , unless viscous effects are considered. The assumption to be used in this work is that the mean flow does have a pressure gradient in the axial direction, due to viscous effects. Notice that for the case of turbulent mean flow, variations of the Reynolds stresses would also produce a streamwise pressure gradient. The other assumption to be used is that there is no axial density gradient for the mean flow. This means that in the equation of state the axial temperature gradient balances an axial pressure gradient. This could happen, for example, due to cooling or heating the flow from the duct walls.

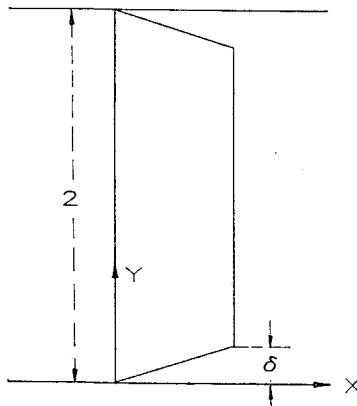


Fig. 1 Flow configuration.

The effects of viscosity on the disturbance flow are neglected. It is assumed that the Reynolds number, based on the ambient speed of sound and the duct width, is large. This is a reasonable assumption to make for the range of frequencies that are of practical interest. Thus, the disturbance flow is governed by the Euler equations. If one substitutes Eqs. (1) into the Euler equations and linearizes, then the Euler equations result in the following system of partial differential equations:

$$[A] \mathbf{q} + [B] \frac{\partial \mathbf{q}}{\partial x} + [C] \frac{\partial \mathbf{q}}{\partial y} = [0] \quad (2a)$$

where

$$\mathbf{q}^T = \{u', v', \rho', p', T'\} \quad (2b)$$

The matrices $[A]$, $[B]$, and $[C]$ are functions of the mean flow quantities. They are defined in the Appendix. The system of Eqs. (2a) needs boundary conditions. However, there is no need to distinguish between different modes of propagation and, therefore, all modes can be accounted for in the solution. In a typical duct acoustics problem, the boundary conditions can be as follows (see Fig. 1).

At the $x=0$ location, the complex impedances f_1 and f_2 are defined as

$$u'/p' = f_1(y) \quad 0 \leq y \leq 2 \quad (3a)$$

$$v'/p' = f_2(y) \quad 0 \leq y \leq 2 \quad (3b)$$

These boundary conditions can be specified, for example, by using measured data for the complex impedance in the x and y directions.

At the end of the duct, the acoustic velocities are prescribed as

$$u'(\ell, y) = f_3(y) \quad 0 \leq y \leq 2 \quad (3c)$$

$$v'(\ell, y) = f_4(y) \quad 0 \leq y \leq 2 \quad (3d)$$

At the rigid duct walls, the no penetration condition dictates that

$$v'(x, 0) = 0 \quad 0 \leq x \leq \ell \quad (3e)$$

$$v'(x, 2) = 0 \quad 0 \leq x \leq \ell \quad (3f)$$

$$\frac{\partial p'}{\partial y}(x, 0) = 0 \quad 0 \leq x \leq \ell \quad (3g)$$

$$\frac{\partial p'}{\partial y}(x, 2) = 0 \quad 0 \leq x \leq \ell \quad (3h)$$

It is true that Eqs. (3g) and (3h) are a result of Eqs. (3e) and (3f). However, it is convenient to use them as separate boundary conditions for the pressure in the numerical treatment of the Euler equations.

It should be mentioned that when isentropic sound propagation is examined, the pressure and density are related. Thus, there is no need to consider the energy equation nor any boundary conditions for the temperature. The above formulation, for the case of no mean flow and under the assumption of a plane acoustic wave, i.e., $v' = 0$, degenerates to the classic piston problem. This problem has a closed form solution as

$$u'(x) = \text{real} \frac{u'(\ell) [if_1(0) \sin \omega x + \cos \omega x]}{\cos \omega \ell + if_1(0) \sin \omega \ell} \quad (4a)$$

$$p'(x) = \text{real} \frac{u'(\ell) [f_1(0) \cos \omega x + i \sin \omega x]}{\cos \omega \ell + if_1(0) \sin \omega \ell} \quad (4b)$$

We next focus attention on the eigenvalue problem. The disturbance flow is treated as periodic in x with the periodicity determined by the wavenumber k . Also, the mean flow is assumed to be parallel. The flow to be examined is

$$u = \bar{u}(y) + Z_1(y) \exp(i\theta) \quad (5a)$$

$$v = Z_2(y) \exp(i\theta) \quad (5b)$$

$$\rho = \bar{\rho} + Z_3(y) \exp(i\theta) \quad (5c)$$

$$p = \bar{p}(x) + Z_4(y) \exp(i\theta) \quad (5d)$$

$$T = T(x) + Z_5(y) \exp(i\theta) \quad (5e)$$

$$\theta = \omega t - kx \text{ or } \theta = \omega t + kx \quad (5f)$$

The disturbance components are composed of an amplitude function that depends on the y coordinate times $\exp(i\omega t - kx)$ for a right-running wave, where ω is the angular real frequency and k the complex wavenumber. If the wave is left running, then the exponential term becomes $\exp(i\omega t + kx)$.

If Eqs. (5) are substituted into the Euler equations, the following system of ordinary differential equations results:

$$[A']Z + [B'] \frac{dZ}{dy} = 0 \quad (6a)$$

$$\{Z\}^T = \{Z_1, Z_2, Z_3, Z_4, Z_5\} \quad (6b)$$

The quantities Z_1, Z_2, Z_3, Z_4, Z_5 are the complex amplitude functions of the disturbance velocities in the x and y directions, disturbance density, pressure, and temperature, respectively. The matrices $[A']$ and $[B']$ are given in the Appendix.

A comparison with previous work is appropriate at this point. If the mean flow is assumed to be isentropic, because of the assumption of fully developed duct flow, the mean density is assumed constant with x . However, the mean pressure is related to the mean density with the isentropic relationship and thus the mean pressure does not depend on x . Therefore, the equation of state dictates that the mean temperature is also invariant with x . The result is that the first three terms on the last row of the matrix $[A']$ become zero because the energy equation for the disturbance flow is simplified. One can then combine the system of Eqs. (6) into the following single equation for the amplitude of the disturbance pressure:

$$\frac{d^2 Z_4}{dy^2} + \left(\frac{2k}{1 - Mk} \right) \frac{dM}{dy} \frac{dZ_4}{dy} + \omega^2 [(Mk - 1)^2 - k^2] Z_4 = 0$$

where M is the mean flow Mach number. This particular equation can also be obtained by assuming a disturbance velocity potential as shown in previous works.^{2,5}

On the solid wall, the boundary condition on the perturbation velocity component in the y direction is zero, because of the no-penetration condition. This, together with the y momentum equation, gives that the y derivative of the acoustic pressure on the wall is zero. The boundary condition for the disturbance temperature is obtained from the energy equation and the boundary condition for the u component of the disturbance velocity from the x momentum equation, with the u component of the mean velocity as zero on the wall. These conditions for a right-running wave are

$$Z_2 = 0 \quad (7a)$$

$$\frac{dZ_4}{dy} = 0 \quad (7b)$$

$$\left(\frac{\bar{\rho}}{\gamma - 1} \frac{\partial \bar{T}}{\partial x} - \frac{\partial \bar{p}}{\partial x} \right) Z_1 = i\omega Z_4 + \frac{i\bar{p}}{\gamma - 1} \omega Z_5 = 0 \quad (7c)$$

$$\omega \bar{\rho} Z_1 - k Z_4 = 0 \quad (7d)$$

All of Eqs. (7) are for $y=0$ where a rigid wall is assumed. These conditions can be applied at both walls if one needs to solve for the whole duct or only at one wall. In the latter case, conditions of symmetry or antisymmetry at the duct center must be imposed, in order to compute the symmetric or antisymmetric modes. In this work, symmetry conditions were used at the center of the duct, namely, that the v disturbance velocity is zero. This forces the y derivative of the disturbance pressure to be zero. The disturbance temperature is obtained from the energy equation.

Therefore, for the center of the duct at $y=1$, we have

$$Z_2 = 0 \quad (8a)$$

$$\frac{dZ_4}{dy} = 0 \quad (8b)$$

$$\left(\frac{\bar{\rho}}{\gamma - 1} \frac{\partial \bar{T}}{\partial x} - \frac{\partial \bar{p}}{\partial x} \right) Z_1 + \frac{u}{\gamma - 1} \frac{\partial T}{\partial x} Z_3 - i\omega (1 - \bar{u}k) Z_4 + \frac{i\rho\omega}{\gamma - 1} (1 - \bar{u}k) Z_5 = 0 \quad (8c)$$

$$\bar{\rho} (\omega - \bar{u}k) Z_1 - k Z_4 = 0 \quad (8d)$$

Because the governing equations (6a) and the boundary conditions are homogeneous, the problem is an eigenvalue problem. Thus, the solution is normalized by setting

$$Z_4(1) = 1 \quad (9)$$

Notice that if the problem for isentropic sound propagation is solved, only Eqs. (7a), (7b), (7d), (8a), (8b), and (8d) are needed in addition to the isentropic relationships.

Numerical Formulation

If one wants to treat the problem described by the system of Eq. (2a) with a spatial marching technique, one can follow the procedure described here. An assumption can be made about the pressure at $x=0$. Then, Eqs. (3a) and (3b) give the acoustic velocity components. Thus, Eqs. (2a) can be integrated in x using a marching procedure. If subscript i denotes the points along x and subscript j the points along y , then the x derivatives for any quantity q can be computed using the following two-point formula, which assumes equal spacing Δx between the points:

$$\frac{\partial q}{\partial x} \Big|_{i,j} = \frac{1}{2\Delta x} (3q_{i,j} - 4q_{i-1,j} + q_{i-2,j}) \quad (10)$$

If the y derivatives are computed using the following central difference formula:

$$\frac{\partial q}{\partial y} \Big|_{i,j} = \frac{1}{2\Delta y} (q_{i,j+1} - q_{i,j-1}) \quad (11)$$

then, assuming the acoustic field is known at the $(i-1)$ and $(i-2)$ locations, the system of Eqs. (2a) can be written as

$$[D]q_{i,j+1} + [E]q_{i,j} + [F]q_{i,j-1} = [G] \quad (12)$$

subject to the boundary conditions [Eqs. (3e) and (3f)]. If one wants to compute the isentropic case, $[D]$, $[E]$, $[F]$,

and $[G]$ are 3×3 matrices, because the isentropic relationships may be used to calculate ρ' and T' . The matrices are given in the Appendix.

A block tridiagonal inversion was used to invert the system of Eq. (12). Two inversion routines were used, one obtained from Ref. 16 and the other written by the authors. The solution can then proceed along x in a spatial marching fashion. A check must be made to see if the final attained acoustic velocities agree with those given by Eqs. (3c) and (3d). If not, the Newton-Raphson iteration procedure may be used to obtain a new guess for the pressure p' at $x=0$ and the procedure must be repeated until this method converges.

For the case of the eigenvalue problem, the system of Eqs. (6a) was discretized in a uniform grid in the y direction (Fig. 1). Second-order accurate, central differences were used. The system of Eq. (6a) can be rewritten as

$$\frac{dZ}{dy} = [C']Z \quad (13)$$

and the discretization gives, at every point i ,

$$[I]Z_{i+1} - 2\Delta y[C'_i]Z_i - [I]Z_{i-1} = 0 \quad (14)$$

where $[I]$ denotes the 5×5 identity matrix. The two block diagonal inversion routines mentioned before produced the same eigenvalues, within the applied tolerance (10 significant digits), on the CDC Cyber 855 computer.

A Newton-Raphson procedure was used on the acoustic pressure to obtain the complex eigenvalue k and, in all cases presented, the tolerance forced the eigenvalue to be accurate in the first 10 digits. The truncation error was checked by computing with varying number of points in the y direction and it was found to be negligible. The procedure has been repeatedly used before.²⁻⁶ The Newton iteration on k results from the fact that not all of the homogeneous boundary conditions are satisfied for a chosen value of k . Thus, Eq. (8b) approaches zero iteratively as k approaches the eigenvalue.

In order to check the solution of the system of Eqs. (2a), the following procedure was used. In the systems of Eqs. (6a) and (14), the energy equation was replaced with the isentropic assumption. Then the eigenvalues obtained were compared with the results of Ref. 4. Very good agreement was found. However because the results from Ref. 4 were read from a graph, this was not considered satisfactory. Therefore the simpler eigenvalue problem [Eq. (7)] was programmed and the resulting eigenvalues were compared with the results obtained using the Euler equations. Again, the obtained eigenvalues agreed to the significant digits imposed by the tolerance used.

Results and Discussion

In order to examine the numerical spatial marching, the piston problem was numerically solved and the answers compared with the closed-form solution described by Eqs. (4).

The explicit marching technique given by Eq. (12) was used to solve the system from left ($x=0.0$) to right ($x=l$, piston location.) Instead of iterating on the upstream pressure, the computations were started with the exact pressure as given by the known analytical solutions [Eq. (4)], attempting to recover the specified acoustic u velocity at the piston end. This was done to check the accuracy of the method. Several runs were made with varying frequencies and grid points. Some representative examples for the nonreflecting ($f_1=1, f_2=0$) case are shown in Fig. 2.

Figure 2 shows that the method is unstable for a large number of grid points in the transverse direction. This is in agreement with the conclusion of Ref. 17, where a similar marching method was used on the Helmholtz equation. For example, for a nondimensional frequency ($\omega l/c$) of 1.0, the most satisfactory result is obtained by using 4 grid points in

the transverse direction and 400 grid points in the axial direction. It may be hypothesized there exists a distinct relationship between Δx , Δy , and the frequency of excitation in order to get meaningful results. The reflecting case ($f \neq 1$) computes more poorly than the nonreflecting case, even with a low number of grid points in the transverse direction.

With the stability limits discussed in Ref. 17, a distinct advantage of this method is that the storage requirements and the computer time required are low. The only quantities that need to be stored are the $q_{i-1,j}$ and $q_{i-2,j}$, in order to compute the $q_{i,j}$.

It is concluded that the restrictions in the mode shape (essentially only plane waves allowed) are too severe for this scheme to be of practical use. Thus, we next turn our attention to the eigenvalue problem. The mean velocity profile shown in Fig. 1 was used in order to compare with the results of Ref. 4 and with the same results obtained from the simplified eigenvalue problem. Figures 3 and 4 show the wavenumber k as a function of the mean flow Mach number, for the lowest mode of propagation, for both upstream (left) and downstream (right) running waves. The results agree well with those of Ref. 5. It may be observed that the wavenumber increases as the mean flow approaches near sonic conditions for the left-running wave, indicating the breakdown of the linear theory of acoustics.

In these calculations, the mean pressure along the duct is constant. The lowest mode propagates unattenuated upstream and downstream and, therefore, the wavenumber is real. Next, various pressure gradients were imposed along the duct. The resulting eigenvalue k contains an imaginary part. For the upstream running waves this imaginary part is plotted for various Mach numbers and pressure gradients in

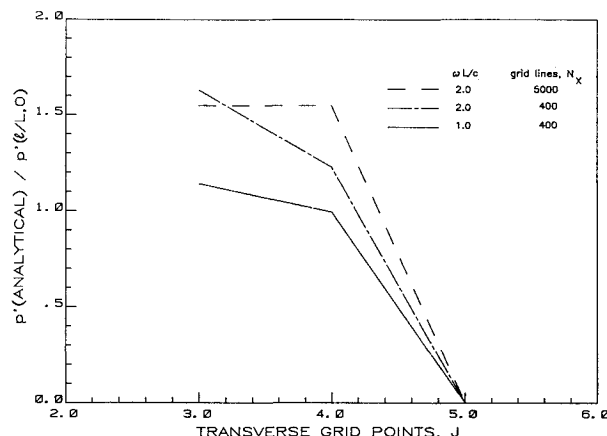


Fig. 2 Numerical stability assessment for the piston problem.

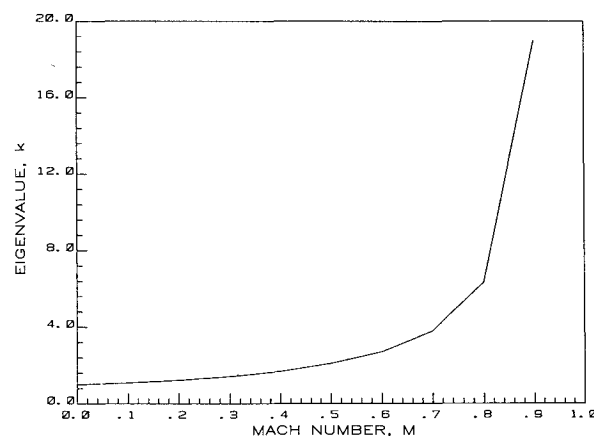


Fig. 3 Lowest mode eigenvalue for a left-running wave.

Fig. 5. It is negative, which implies that the wave is attenuated. However, for downstream propagating waves the eigenvalue has a positive imaginary part (Fig. 6). Therefore, the wave grows unstable as it propagates downstream. This instability is due to the inclusion of the full energy equation, with the pressure and temperature gradients on the mean flow.

The difference between the pressure of the acoustic wave when it is considered isentropic and the one computed in this paper is very small, as can be seen in Table 1. Therefore, it would be very difficult to distinguish between the two in an experiment. Also, the real part of the wavenumber and, hence, the propagation speed is the same to the third significant digit. Therefore, there is essentially no dispersion because of the new eigenvalue relationships (generated numerically).

It should be also mentioned that the computed instability is not of the "critical-layer" type because the phase speed is higher than the mean flow velocities. This is the reason that we restricted our attention to the lowest mode, so that the geometry does not play any role. It seems that the instability is due to the inclusion of the full energy equation. However, for a ramjet combustor, heat sources or sinks (cold walls) can have similar effects and result in the same type of instability.

The flow was strictly parallel with mean density being independent of the streamwise coordinate and with a favorable

pressure gradient. In order for this to be true, the equation of state dictates that dT/dx ought to be negative. Actual values for dT/dx were obtained from dP/dx and the state equation.

The instability of the acoustic wave we computed is due to the fact that the nonisentropic sound propagation is com-

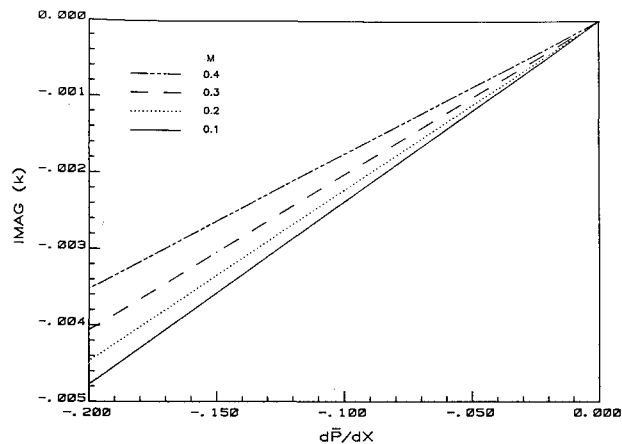


Fig. 5 Imaginary part of eigenvalue for a left-running wave.

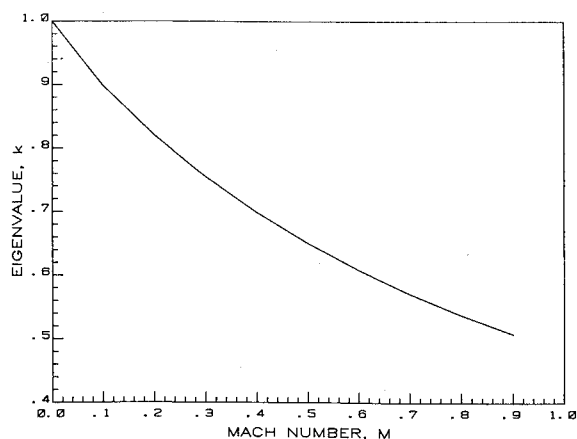


Fig. 4 Lowest mode eigenvalue for a right-running wave.

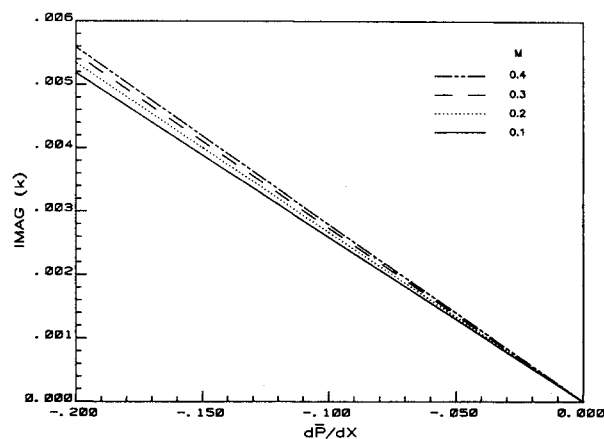


Fig. 6 Imaginary part of eigenvalue for a right-running wave.

Table 1 Results for a linear boundary-layer profile for half-duct width ($M=0.4$)

$dP/dx = 0.0$			$dP/dx = -0.2$		
Y	Real p	Imag p	Y	Real p	Imag p
0.000	-0.3626E+00	0.	0.000	-0.3625E+00	-0.1015E-02
0.050	-0.2931E+00	0.	0.050	-0.2931E+00	-0.9300E-03
0.100	-0.1835E+00	0.	0.100	-0.1834E+00	-0.8402E-03
0.150	-0.8648E-01	0.	0.150	-0.8642E-01	-0.8035E-03
0.200	0.1134E-01	0.	0.200	0.1139E-01	-0.7583E-03
0.250	0.1090E+00	0.	0.250	0.1091E+00	-0.7060E-03
0.300	0.2057E+00	0.	0.300	0.2058E+00	-0.6480E-03
0.350	0.3004E+00	0.	0.350	0.3004E+00	-0.5856E-03
0.400	0.3922E+00	0.	0.400	0.3923E+00	-0.5205E-03
0.450	0.4803E+00	0.	0.450	0.4803E+00	-0.4541E-03
0.500	0.5637E+00	0.	0.500	0.5638E+00	-0.3878E-03
0.550	0.6418E+00	0.	0.550	0.6418E+00	-0.3232E-03
0.600	0.7137E+00	0.	0.600	0.7137E+00	-0.2615E-03
0.650	0.7788E+00	0.	0.650	0.7788E+00	-0.2040E-03
0.700	0.8364E+00	0.	0.700	0.8364E+00	-0.1518E-03
0.750	0.8860E+00	0.	0.750	0.8860E+00	-0.1061E-03
0.800	0.9271E+00	0.	0.800	0.9271E+00	-0.6774E-04
0.850	0.9593E+00	0.	0.850	0.9593E+00	-0.3742E-04
0.900	0.9823E+00	0.	0.900	0.9823E+00	-0.1577E-04
0.950	0.9959E+00	0.	0.950	0.9959E+00	-0.3215E-05
1.000	0.1000E+01	0.	1.000	0.1000E+01	0.

puted. Therefore, the instability falls into the category of combustion instability.¹⁵ Attention was confined to the lowest mode because, for combustion problems, it appears more often than the higher modes. The existence of higher modes of instability and their interaction, in the presence of various mean flow effects, is a subject for further research.

Appendix

The matrices $[A]$, $[B]$, and $[C]$ are given as follows:

$$\begin{aligned}
 a_{11} &= \frac{\partial \bar{p}}{\partial x} & a_{12} &= \frac{\partial \bar{p}}{\partial y} \\
 a_{13} &= \frac{\partial \bar{u}}{\partial x} + \frac{\partial \bar{v}}{\partial y} + i\omega & a_{21} &= \bar{p} \frac{\partial \bar{u}}{\partial x} + \bar{p} i\omega \\
 a_{22} &= \bar{p} \frac{\partial \bar{u}}{\partial y} & a_{23} &= \frac{\bar{u} \partial \bar{u}}{\partial x} + \frac{\bar{v} \partial \bar{u}}{\partial y} \\
 a_{31} &= \bar{p} \frac{\partial \bar{v}}{\partial x} & a_{32} &= \bar{p} \frac{\partial \bar{v}}{\partial y} + \bar{p} i\omega \\
 a_{33} &= \frac{\bar{u} \partial \bar{v}}{\partial x} + \frac{\bar{v} \partial \bar{v}}{\partial y} & a_{43} &= -1/\bar{p} \\
 a_{44} &= 1/\bar{p} & a_{45} &= -1/\bar{T} \\
 a_{51} &= \frac{\bar{p}}{\gamma-1} \frac{\partial \bar{T}}{\partial x} - \frac{\partial \bar{p}}{\partial x} & a_{52} &= \frac{\bar{p}}{\gamma-1} \frac{\partial \bar{T}}{\partial y} - \frac{\partial \bar{p}}{\partial y} \\
 a_{53} &= \frac{1}{\gamma-1} \left(\frac{\bar{u} \partial \bar{T}}{\partial x} + \frac{\bar{v} \partial \bar{T}}{\partial y} \right) \\
 a_{54} &= -i\omega & a_{55} &= \bar{p} i\omega / \gamma - 1 \\
 a_{14} &= a_{15} = a_{24} = a_{25} = a_{34} = a_{35} = a_{41} = a_{42} = 0 \\
 b_{11} &= \bar{p} & b_{13} &= \bar{u} \\
 b_{21} &= \bar{p} \bar{u} & b_{24} &= 1 \\
 b_{32} &= \bar{p} \bar{v} & & \\
 b_{54} &= -\bar{u} & b_{55} &= \bar{p} \bar{u} / \gamma - 1 \\
 b_{12} &= b_{14} = b_{15} = b_{22} = b_{23} = b_{25} = b_{31} = b_{33} = b_{34} = b_{35} = 0 \\
 b_{41} &= b_{42} = b_{43} = b_{44} = b_{45} = b_{51} = b_{52} = b_{53} = 0 \\
 c_{12} &= \bar{p} & c_{13} &= \bar{v} \\
 c_{21} &= \bar{p} \bar{v} & & \\
 c_{32} &= \bar{p} \bar{v} & c_{34} &= 1 \\
 c_{54} &= -\bar{v} & c_{55} &= \bar{p} \bar{v} / \gamma - 1 \\
 c_{11} &= c_{14} = c_{15} = c_{22} = c_{23} = c_{24} = c_{25} = c_{31} = c_{33} = c_{35} = 0 \\
 c_{41} &= c_{42} = c_{43} = c_{44} = c_{45} = c_{51} = c_{52} = c_{53} = 0
 \end{aligned}$$

The matrices $[A']$ and $[B']$ are given as follows:

$$\begin{aligned}
 a'_{11} &= \bar{p} i k \omega & a'_{13} &= i\omega (1 + k\bar{u}) \\
 a'_{21} &= \bar{p} i\omega (1 + k\bar{u}) & a'_{22} &= \bar{p} \frac{\partial \bar{u}}{\partial y}
 \end{aligned}$$

$$\begin{aligned}
 a'_{24} &= i k \omega & a'_{32} &= \bar{p} i\omega (1 + k\bar{u}) \\
 a'_{43} &= -1/\bar{p} & a'_{44} &= 1/\bar{p} \\
 a'_{45} &= -1/\bar{T} & a'_{51} &= \frac{\bar{p}}{\gamma-1} \frac{\partial \bar{T}}{\partial x} - \frac{\partial \bar{p}}{\partial x} \\
 a'_{53} &= \frac{\bar{u}}{\gamma-1} \frac{\partial \bar{T}}{\partial x} & a'_{54} &= -i\omega (1 + k\bar{u}) \\
 a'_{55} &= \frac{\bar{p} i\omega}{\gamma-1} (1 + k\bar{u}) \\
 a'_{12} &= a'_{14} = a'_{15} = a'_{23} = a'_{25} = a'_{31} = a'_{33} = a'_{34} = a'_{35} = 0 \\
 a'_{41} &= a'_{42} = a'_{52} = 0 \\
 b'_{12} &= \bar{p} & b'_{34} &= 1 \\
 b'_{11} &= b'_{13} = b'_{14} = b'_{15} = b'_{21} = b'_{22} = b'_{23} = b'_{24} = b'_{25} = 0 \\
 b'_{31} &= b'_{32} = b'_{33} = b'_{35} = b'_{41} = b'_{42} = b'_{43} = b'_{44} = b'_{45} = 0 \\
 b'_{51} &= b'_{52} = b'_{53} = b'_{54} = b'_{55} = 0
 \end{aligned}$$

The matrices $[D]$, $[E]$, $[F]$, and $[G]$ are as follows:

$$\begin{aligned}
 [D] &= \frac{1}{2\Delta y} [C] \\
 [E] &= [A] + \frac{3[B]}{2\Delta x} \\
 [F] &= -\frac{1}{2\Delta y} [C] \\
 [G] &= \frac{(4q_{i-1,j} - q_{i-2,j}) [B]}{2\Delta x}
 \end{aligned}$$

Acknowledgment

This work was supported by the U.S. Office of Naval Research under Contract N00014-84-K0293.

References

- Davis, J. A., Komerath, N. M., Walterick, R. E., Strahle, W. C., and Lekoudis, S. G., "Acoustic Behavior of the Solid Fuel Ramjet Simulator," AIAA Paper 86-0003, 1986.
- Pridmore-Brown, D. C., "Sound Propagation in a Fluid Flowing Through an Attenuation Duct," *Journal of Fluid Mechanics*, Vol. 14, 1958, pp. 393-406.
- Mungur, P. and Gladwell, G. M. L., "Acoustic Wave Propagation in a Sheared Flow Contained in a Duct," *Journal of Sound and Vibration*, Vol. 9, 1969, pp. 28-48.
- Nayfeh, A. H., Kaiser, J. H., and Telionis, D. P., "Acoustics of Aircraft Engine-Duct Systems," *AIAA Journal*, Vol. 13, Feb. 1975, pp. 130-153.
- Savkar, S. D., "Propagation of Sound in Ducts with Shear Flow," *Journal of Sound and Vibration*, Vol. 19, No. 3, 1971, pp. 355-372.
- Nayfeh, A. H., Telionis, D. P., and Lekoudis, S. G., "Acoustic Propagation in Ducts with Varying Cross Sections and Sheared Mean Flow," AIAA Paper 73-1008, 1973.
- Baumeister, K. H., Eversman, W., Astley, R. J., and White, J. W., "Acoustics in Variable Area Duct: Finite Element and Finite Difference Comparisons to Experiment," *AIAA Journal*, Vol. 21, Feb. 1983, pp. 193-199.
- Quinn, D. W., "Finite Difference Method for Computing Sound Propagation in Nonuniform Ducts," *AIAA Journal*, Vol. 13, Oct. 1975, pp. 1392-1394.

⁹Alfredson, R. J., "The Propagation of Sound in a Circular Duct of Continuously Varying Cross-Sectional Area," *Journal of Sound and Vibration*, Vol. 23, No. 4, 1972, pp. 433-442.

¹⁰Nayfeh, A. H., Kaiser, J. E., and Shaker, B. S., "A Wave-Envelope Analysis of Sound Propagation in Nonuniform Circular Ducts with Compressible Mean Flows," NASA CR-3109, March 1979.

¹¹Baumeister, K. J. and Rice, E. J., "A Difference Theory for Noise Propagation in an Acoustically Lined Duct with Mean Flow," *AIAA Progress in Astronautics and Aeronautics: Aeronautics: Jet and Combustion Noise Duct Acoustics*, Vol. 37, edited by H. T. Nagamatsu, J. V. O'Keefe, and I. R. Schwartz, AIAA, New York, 1975, pp. 435-453.

¹²Abrahamson, A. L., "A Finite Element Algorithm for Sound Propagation in Axisymmetric Ducts Containing Compressible Mean Flow," AIAA Paper 77-1301, Oct. 1977.

¹³Hariharan, S. I., "Numerical Solutions of Acoustic Wave Propagation Problems Using Euler Computations," AIAA Paper 84-2290, Oct. 1984.

¹⁴Maestrello, L., Bayliss, A., and Turkel, E., "On the Interaction of a Sound Pulse with the Shear Layer of an Axisymmetric Jet," *Journal of Sound and Vibration*, Vol. 74, No. 2, 1981, pp. 281-301.

¹⁵*Liquid Propellant Rocket Combustion Instability*, NASA SP-194, 1972.

¹⁶Anderson, D. A., Tannehill, J. C., and Pletcher, R. H., *Computational Fluid Mechanics and Heat Transfer*, McGraw-Hill Book Co., New York, 1984.

¹⁷Baumeister, K. H., "Numerical Spatial Marching Techniques in Duct Acoustics," *Journal of the Acoustical Society of America*, Vol. 65, No. 2, 1979, pp. 297-306.

From the AIAA Progress in Astronautics and Aeronautics Series . . .

GASDYNAMICS OF DETONATIONS AND EXPLOSIONS—v. 75 and COMBUSTION IN REACTIVE SYSTEMS—v. 76

*Edited by J. Ray Bowen, University of Wisconsin,
N. Manson, Université de Poitiers,
A. K. Oppenheim, University of California,
and R. I. Soloukhin, BSSR Academy of Sciences*

The papers in Volumes 75 and 76 of this Series comprise, on a selective basis, the revised and edited manuscripts of the presentations made at the 7th International Colloquium on Gasdynamics of Explosions and Reactive Systems, held in Göttingen, Germany, in August 1979. In the general field of combustion and flames, the phenomena of explosions and detonations involve some of the most complex processes ever to challenge the combustion scientist or gasdynamicist, simply for the reason that *both* gasdynamics and chemical reaction kinetics occur in an interactive manner in a very short time.

It has been only in the past two decades or so that research in the field of explosion phenomena has made substantial progress, largely due to advances in fast-response solid-state instrumentation for diagnostic experimentation and high-capacity electronic digital computers for carrying out complex theoretical studies. As the pace of such explosion research quickened, it became evident to research scientists on a broad international scale that it would be desirable to hold a regular series of international conferences devoted specifically to this aspect of combustion science (which might equally be called a special aspect of fluid-mechanical science). As the series continued to develop over the years, the topics included such special phenomena as liquid- and solid-phase explosions, initiation and ignition, nonequilibrium processes, turbulence effects, propagation of explosive waves, the detailed gasdynamic structure of detonation waves, and so on. These topics, as well as others, are included in the present two volumes. Volume 75, *Gasdynamics of Detonations and Explosions*, covers wall and confinement effects, liquid- and solid-phase phenomena, and cellular structure of detonations; Volume 76, *Combustion in Reactive Systems*, covers nonequilibrium processes, ignition, turbulence, propagation phenomena, and detailed kinetic modeling. The two volumes are recommended to the attention not only of combustion scientists in general but also to those concerned with the evolving interdisciplinary field of reactive gasdynamics.

*Published in 1981, Volume 75—446 pp., 6×9, illus., \$35.00 Mem., \$55.00 List
Volume 76—656 pp., 6×9, illus., \$35.00 Mem., \$55.00 List*

TO ORDER WRITE: Publications Dept., AIAA, 1633 Broadway, New York, N.Y. 10019